Organic & Biomolecular Chemistry

Cite this: *Org. Biomol. Chem.*, 2011, **9**, 5156

www.rsc.org/obc

PAPER

Domino synthesis of 1,3,5-trisubstituted hydantoins: a DFT study†

Tommaso Marcelli,* Francesca Olimpieri and Alessandro Volonterio*

Received 15th February 2011, Accepted 3rd May 2011
DOI: 10.1039/c1ob05242j

The mechanism of the reaction between carbodiimides and activated α,β-unsaturated carboxylic acids yielding fully substituted hydantoins and variable amounts of *N*-acyl urea by-products was studied using density functional theory calculations. Two alternative pathways featuring *N*-acyl ureas and imino-oxazolidinones as intermediates for the formation of the hydantoin product were taken into account. The results obtained using two different computational models indicate that the overall barriers are similar for the two pathways considered. In all cases, inclusion of a second molecule of carboxylic acid was required to mediate tautomerizations and rearrangement steps. The calculations successfully reproduce the experimentally observed regioselectivity with respect to both *N*-acyl urea and hydantoin products.

Introduction

Small functionalized heterocycles play a central role in medicinal chemistry.[1] A large number of either synthetic or naturally occurring compounds showing high biological activities contain heterocyclic rings. Furthermore, such rigidified scaffolds act as valuable building blocks in the development of novel pharmaceuticals, since they can often be readily functionalised with a variety of pharmacophoric groups.

In this respect, hydantoins represent a very important class of biologically active heterocyclic compounds, as testified by their broad medicinal and agrochemical applications. Many hydantoin derivatives have been identified as anticonvulsants and antimuscarinics, antiulcers and antiarrythmics, antivirals, antidiabetics, serotonin and fibrinogen receptor antagonists, inhibitors of the glycine binding site of NMDA receptors and anticancer.[2] Furthermore, substituted hydantoins may afford non-natural α-amino acids *via* alkaline hydrolytic degradation,[3] eventually in optically pure form if submitted to dynamic kinetic resolution.[4] Thus, the chemistry of multiple substituted hydantoins has been extensively investigated during the years.

Such compounds are traditionally prepared by cyclization in strongly acidic or basic media of ureido acids, obtained from the reaction of α-amino acids or amino nitriles with alkyl, aryl, or chlorosulfonyl isocyanates, respectively, which require extended reaction times or high temperatures.[5] Furthermore, only 3,5-di- and 3,5,5-trisubstituted hydantoins are readily accessible in this way, while a preliminary alkylation of the amino moiety, by reductive amination or *via* Mitsunobu reaction, is required in order to achieve the synthesis of fully substituted hydantoins.[6] Alternative methodologies, reported in the past years for the preparation of 1,3,5-trisubstituted hydantoins, include a palladium-catalyzed one-pot carbonylation of aldehydes in the presence of urea derivatives,[7] a novel application of the Ugi five-component condensation[8] and a base-catalyzed rearrangement of 5-substituted barbituric acids.[9] Efficient protocols for the preparation of hydantoins on solid supports are also known.[10]

In this context, our group recently developed a straightforward and atom-efficient protocol for the one-pot synthesis of hydantoins from carbodiimides and activated α,β-unsaturated carboxylic acids (Scheme 1).[11]

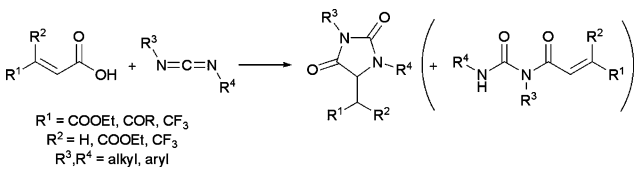

Scheme 1 Domino synthesis of 1,3,5-trisubstituted hydantoins.

This approach allowed the synthesis of a variety of heterocyclic derivatives with mostly good yields and high regioselectivity. In some cases, formation of the desired product was accompanied by substantial amounts of *N*-acyl ureas. Nevertheless, variation of the reaction conditions (addition of a stoichiometric base and/or use of a different solvent) allowed isolation of the target compounds in good yields for nearly all the combination of reaction partners. Interestingly, both hydantoins and *N*-acyl ureas are often formed with complete regioselectivity. In addition, we could detect small amounts of *N*-acyl ureas even for high-yielding substrate combinations. While the synthetic protocols for this reaction have been described considering reaction times of several hours, ^{1}H-NMR analysis of a reaction mixture immediately after mixing of the reactants was inconclusive, in that we were not

Dipartimento di Chimica, Materiali ed Ingegneria Chimica "Giulio Natta", Politecnico di Milano, Via Mancinelli 7, 20131, Milano, Italy. E-mail: tommaso.marcelli@chem.polimi.it, alessandro.volonterio@polimi.it; Fax: +39 02 2399 3080; Tel: +39 02 2399 3056

† Electronic supplementary information (ESI) available: Cartesian coordinates and energies for all stationary points. See DOI: 10.1039/c1ob05242j

able to detect intermediates or observe significant variations over time. In this contribution, we present a theoretical study of the title reaction using high-level density functional theory calculations aimed at obtaining insights into the mechanism of this transformation.

Computational methods

All calculations were performed using the *Gaussian03* package.[12] The stationary points were fully optimized in the gas phase using the B3LYP[13] density functional with the 6-31G(d,p) basis set and subsequently confirmed by vibrational analysis. When necessary, different diastereomeric arrangements were taken into account in the location of the stationary points. For convenience, only the lowest-energy ones are discussed in the text. The nature of the transition states was studied either by visualization of the vibration corresponding to the only imaginary frequency or by intrinsic reaction coordinate scans. Single-point energies were then calculated with both the B3LYP and the MPW1K[14] functionals, using the larger 6-311+G(2d,2p) basis set. Solvent effects were taken into account by performing single-point calculations on the optimized structures with the CPCM[15] continuum solvation model at the B3LYP/6-31G(d,p) level of theory, using $\varepsilon = 8.93$ for dichloromethane. The final energies were obtained by adding the zero-point vibrational correction and the CPCM total electrostatic correction to the electronic energies calculated with the larger basis set. The two potential energy surfaces obtained using the different functionals are fairly similar, although there is significant disagreement with respect to the nature of the rate-determining steps. Unless otherwise stated, the energies reported in the main text have been calculated using the B3LYP functional, as these results compare better with the available experimental data (see below). The potential energy profiles obtained with MPW1K are available in the ESI.†The representations of the stationary points were produced using *CYLview*.[16]

Mechanistic hypothesis

The initial evaluation of the various mechanistic pathways to product formation was performed using a small computational model composed of acid **1a** and dimethylcarbodiimide **2** (Scheme 2).

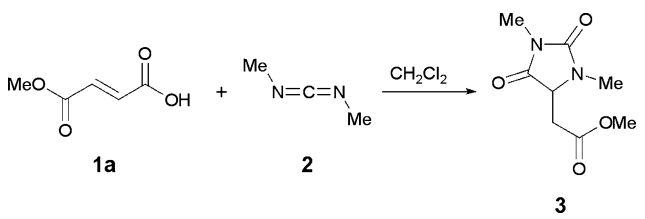

Scheme 2 Computational model.

Next to the obvious advantages in terms of computational costs, the use of a small symmetrical carbodiimide allowed regiochemical aspects of this reaction to be considered separately (see below). In an early stage of this project, inclusion of a second molecule of acid **1a** in the computational model was found to be essential for proton shuttling in conjugate addition and tautomerization steps. Moreover, the calculations show how a carboxylic acid could promote the rearrangement of an intermediate imino-oxazolidinone to the thermodynamically more stable hydantoin product.

The reaction of carboxylic acids with carbodiimides constitutes the basis of several peptide coupling protocols and it is known to proceed *via* an *O*-acylisourea intermediate.[17] One of the main problems of this approach to amide bond synthesis is represented by the tendency of *O*-acyl isoureas to rearrange to the considerably more stable *N*-acyl ureas. In amide couplings, this problem is often overcome by using catalytic amounts of strong nucleophiles which are capable of creating a second highly electrophilic species with no risk of degradation.[18] The mechanistic possibilities which were scrutinized in this work are depicted in Scheme 3. In principle, intramolecular conjugate addition might take place from the *O*-acyl isourea intermediate **4**, instead of the 1,3-acyl shift required for the formation of the *N*-acyl urea. In this case, the addition product would be imino-oxazolidinone **5**, which is known to quickly rearrange to the more stable hydantoin upon treatment with an aqueous base (Pathway A).[19] However, the mechanism for this transformation is not known and the previously proposed 1,3-acyl shift[11] cannot take place due to geometric constraints. Alternatively, *N*-acyl urea **6** might be an intermediate in the formation of the desired product. In this respect, one of the nitrogen atoms could act as nucleophile in a conjugate addition to the α,β-unsaturated ester moiety and generate the hydantoin heterocycle (Pathway B). Also in this case, literature precedents[20] as well as our own experience[21] testify the feasibility of this reaction using a weak base in a protic medium.

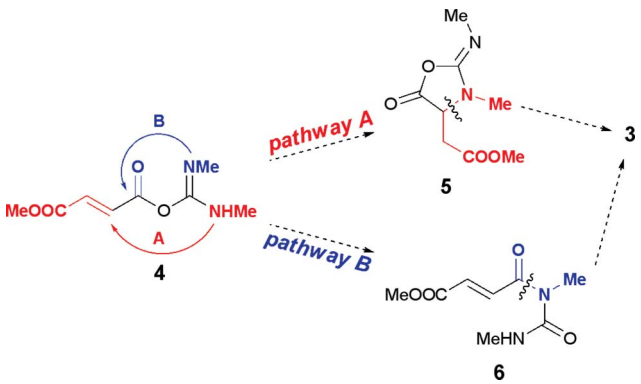

Scheme 3 Mechanistic pathways considered in this study.

Results and discussion

Pathway A

The sequence of elementary steps involved in Pathway A is depicted in Scheme 4 while the geometry of selected transition states is given in Fig. 1. Both pathways begin with a concerted proton transfer–nucleophilic addition ($\mathbf{TS_1}$), which was calculated to be a fast step. Repeated transition state optimizations starting from different guess geometries consistently converged to $\mathbf{TS_1}$, which leads to the formation of a *Z*-isourea. We note that the geometry of this six-membered transition state resembles previously described saddle points for the hydrolysis of carbodiimide with two molecules of water.[22] Also in these cases, the transition states clearly lead to the formation of a *Z*-imine. A possible explanation

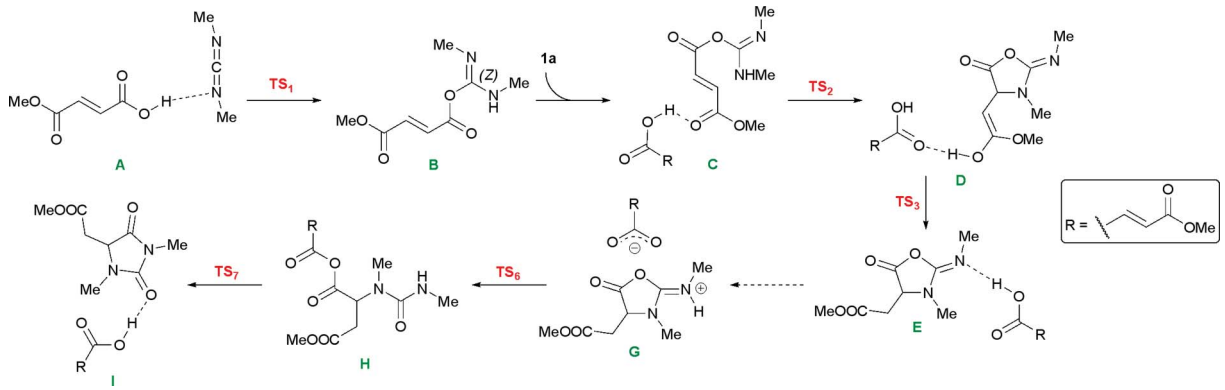

Scheme 4 Pathway A: aza-Michael addition and imino-oxazolidinone rearrangement.

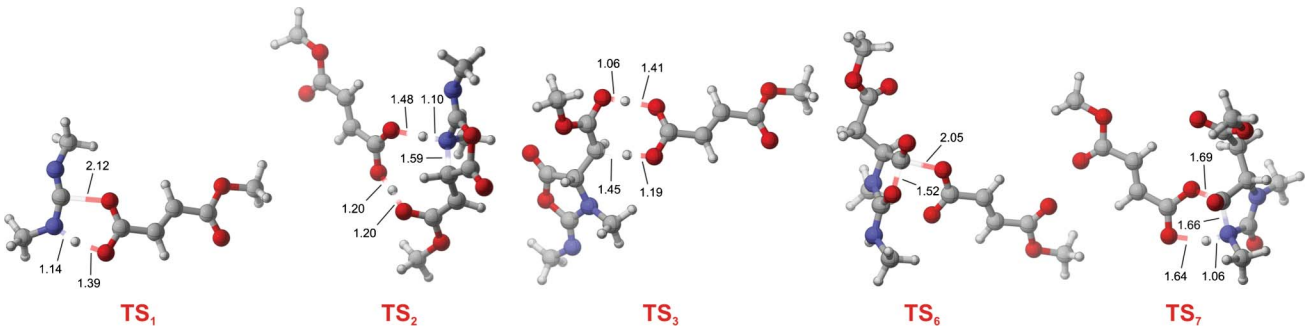

Fig. 1 Transition states in Pathway A.

for this phenomenon might involve repulsion between the lone pairs on the carbodiimide nitrogen and the carboxylate oxygen, which is minimized in the transition state leading to the *Z*-product. A somewhat similar behaviour was observed in nucleophilic additions to isocyanides[23] and rationalized by Nguyen and co-workers in terms of stereoelectronic effects.[24]

Coordination of a second molecule of acid **1a** yields structure **C**, featuring a hydrogen bond between the carboxylic acid moiety of **1a** and the ester of the isourea. This arrangement allows proton shuttling in the following conjugate addition step ($\mathbf{TS_2}$), which closes the five-membered ring. A second proton transfer takes place in $\mathbf{TS_3}$, resulting in the tautomerization of structure **D** to the significantly more stable imino-oxazolidinone.[25]

Next, we addressed the mechanism for the conversion of the imino-oxazolidinone intermediate **5** to the hydantoin product **3**. We envisioned that this formal 1,3 O→N acyl shift, which requires a sequential ring-opening/ring-closure, could be promoted by the reversible nucleophilic addition of the carboxylate of compound **1a**. In this scenario, a mixed anhydride would be the acyl donor reacting with one of the urea nitrogens to yield the hydantoin ring. The first step of this sequence requires protonation of the imine moiety of compound **5**, yielding the required carboxylate as well as a sufficiently electrophilic heterocycle for the subsequent nucleophilic addition. In this respect, several attempts to locate a transition state for proton transfer to the imine nitrogen were unsuccessful. However, we managed to locate an alternative pathway from **E** to **G**, involving the formation of a temporary C–O bond between the carboxylate oxygen and the imine carbon (see Scheme S1 in the ESI†). This is most likely a computational artefact and we ascribe it mainly to the shortcomings of DFT (and the B3LYP functional in particular)[26] in the optimization of stationary points with significant charge separation. For this reason, these results are not discussed further.

Starting from structure **G**, ring-opening *via* attack of the carboxylate to the oxazolidinone carbonyl ($\mathbf{TS_6}$) was calculated to be a facile process. The following ring-closure to the hydantoin product is accompanied by proton transfer to the carboxylate ($\mathbf{TS_7}$), hence liberating product **3** and carboxylic acid **1**. This last step was found to be the most energetically demanding one with respect to the imidazolidinone rearrangement.

Fig. 2 summarizes the calculated energy profile for Pathway A using the B3LYP functional. From these data, the conjugate addition leading to the first ring-closure is predicted to be rate determining, with an overall barrier of 22.7 kcal mol^{-1} ($\mathbf{A}\rightarrow\mathbf{TS_2}$). On the other hand, the highest barrier predicted by MPW1K

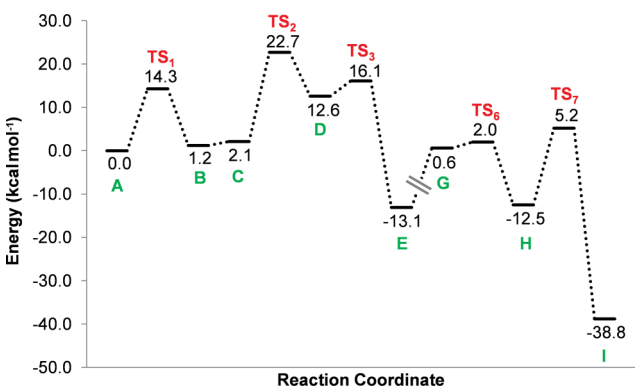

Fig. 2 Potential energy profile for Pathway A.

involves the final step of the ring rearrangement (**H**→**TS**$_7$, 18.7 kcal mol^{-1}).

Pathway B

In this second mechanistic hypothesis, the intermediate *O*-acyl isourea rearranges to the more stable *N*-acyl urea and the hydantoin ring is formed by an aza-Michael addition (Scheme 5); relevant transition states are depicted in Fig. 3.

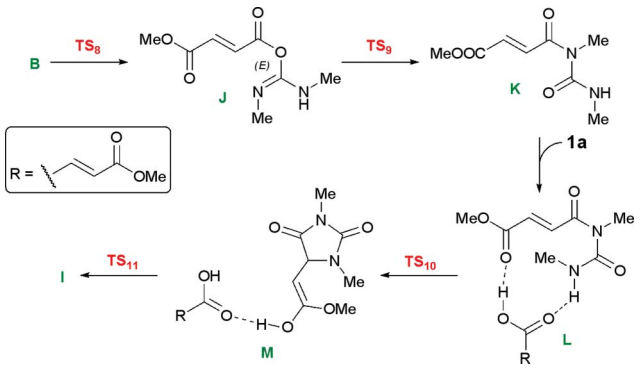

Scheme 5 Pathway B: O→N acyl shift and aza-Michael addition.

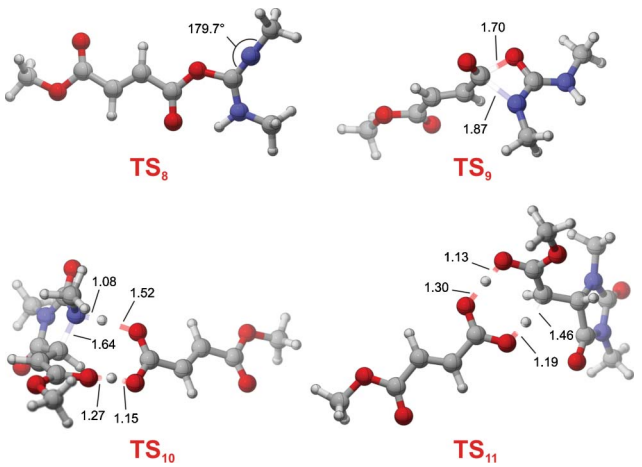

Fig. 3 Transition states in Pathway B.

Z-**4** cannot undergo 1,3 O→N acyl transfer due to geometric constraints, therefore we optimized a transition state for the thermal *E*/*Z* isomerisation of the *O*-acyl isourea (**TS**$_8$). The barrier for this transformation was calculated to be appreciably higher than for the previous step and isourea *E*-**4** was found to be less stable than its *Z* isomer by 1.3 kcal mol^{-1}. On the other hand, the subsequent 1,3 O→N acyl transfer was found to be a very fast process, with the formation of *N*-acyl urea **6** being accompanied by a significant thermodynamic gain. This transformation is a pseudopericyclic rearrangement, which takes place through a concerted four-membered transition state (**TS**$_9$) featuring simultaneous C–O dissociation and C–N bond formation, in agreement with previous computational studies on related transformations.[23,27] While the calculations reported here address the behaviour of a specific type of carboxylic acid and should not be uncritically extrapolated to other systems, our results shed light on some aspects of carbodiimide-mediated amide couplings. In particular, the predicted stereoselectivity in the formation of *O*-acyl isoureas indicates that *E*/*Z* isomerisation of the C=N double bond could be a relevant process for the formation of the undesired *N*-acyl urea product.

Similar to what was described for Pathway A, in this case we found that inclusion of a second molecule of acid **1a** in the computational model was crucial to locate the stationary points leading to the formation of the hydantoin product. Hence, the arrangement of the bimolecular complex found in structure **L** allows a urea proton to be shuttled to the ester moiety in the subsequent conjugate addition step (**TS**$_{10}$). This is followed by an acid-assisted tautomerization of the enol ether (**TS**$_{11}$) to hydantoin **3** and acid **1a**.

The potential energy profile for Pathway B calculated with B3LYP (Fig. 4) indicates that formation of *N*-acyl urea **6** is a rather facile process for the system considered and that the energetically most demanding step is the conjugate addition closing the hydantoin ring, with an overall barrier of 20.2 kcal mol^{-1} (**K**→**TS**$_{10}$). Instead, MPW1K predicts *E*/*Z* isomerization of the *O*-acyl isourea (**B**→**TS**$_8$) to have the highest barrier (18.7 kcal mol^{-1}) in the sequence of steps considered.

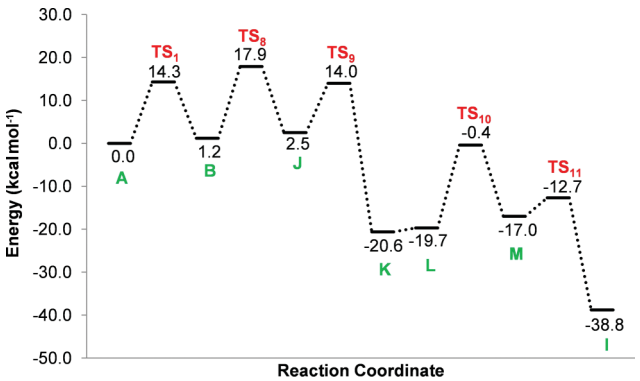

Fig. 4 Potential energy profile for Pathway B.

Therefore, B3LYP indicate a moderate yet significant preference for Pathway B (2.5 kcal mol^{-1}). Instead, MPW1K predicts both pathways to have identical overall barriers. As mentioned above, the two density functionals give significantly different results with respect to the rate-determining steps for each pathway. MPW1K predicts the formation of the postulated intermediate **5** to be a very easy process, while its conversion to hydantoin **3** would be energetically more demanding. For the transformation studied here, we note that imino-oxazolidinone **5** was never isolated or detected spectroscopically by ^{1}H-NMR analysis of the reaction mixture. Likewise, the MPW1K potential energy profile for Pathway B indicates that the formation of *N*-acyl urea **6** is significantly more challenging than its subsequent cyclization to the hydantoin product. Again, this is not in agreement with the observation of occasionally substantial amounts of *N*-acyl urea by-products in the reaction. On the other hand, the qualitative trend obtained from the B3LYP energies is opposite and in better agreement with the available experimental data: 1) rate-determining formation of imino-oxazolidinone **5** and easy ring rearrangement to hydantoin **3** in Pathway A; 2) facile formation of *N*-acyl urea **6** and rate-determining cyclization to the final product in Pathway B.

Larger model

As the carbodiimides routinely employed for this reaction are considerably larger than compound **2** and the steric interactions in some of the steps described above might significantly alter the two potential energy profiles, we performed additional calculations with the B3LYP functional using a larger model, also in order to address the regioselectivity of the reaction.

Starting from the calculated structures described above, we optimized selected stationary points for both pathways using a computational system composed of acid **1a** and unsymmetrical carbodiimide **7**. This substrate combination was chosen based on the complete regioselectivity observed experimentally with acid **1b** in the formation of both hydantoin and *N*-acyl urea (Scheme 6). In order to reduce the conformational complexity of the system as well as its computational cost, in these calculations a molecule of acetic acid, rather than compound **1a**, was used for proton shuttling.

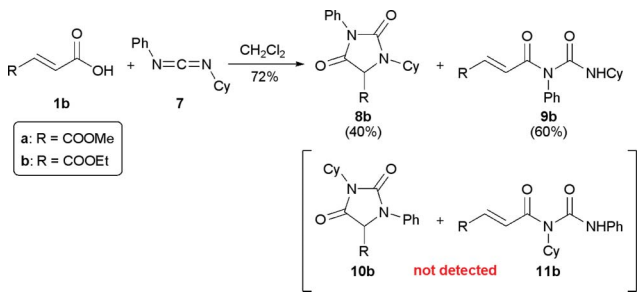

Scheme 6 Regioselectivity with an unsymmetrical carbodiimide.

We first addressed the overall regioselectivity of the reaction which is decided in the ring closure step to the imino-oxazolidinone for Pathway A ($\mathbf{TS_2}$) and in the 1,3 O→N acyl transfer step for Pathway B ($\mathbf{TS_9}$). By doing so, we assumed that the two tautomeric *O*-acyl isoureas resulting from the reaction of acid **1a** and carbodiimide **7** could rapidly interconvert. According to our mechanistic hypothesis, in Pathway B, cyclization of *N*-acyl urea **9** would yield hydantoin **8** while compound **11** would be converted to the regioisomeric heterocycle **10**.[28] For both pathways, the computational predictions are in agreement with the experimentally observed selectivity.

The lowest-energy transition states leading to the formation of the two regioisomeric imino-oxazolidinones are depicted in Fig. 5.[29] The calculations predict a strong preference for $\mathbf{TS_{2\text{-}Ph}}$, ultimately leading to hydantoin **8a**. The geometries of the two structures are rather similar, with $\mathbf{TS_{2\text{-}Cy}}$ being a relatively early transition state compared to $\mathbf{TS_{2\text{-}Ph}}$, as can be observed by the difference in the key C–N distance. Nevertheless, inspection of interatomic contacts did not reveal significant steric interactions in either transition state. In this respect, the strong preference for $\mathbf{TS_{2\text{-}Ph}}$ seems to originate from the increased nucleophilicity of the nitrogen atom bearing an aliphatic substituent.

Also in the case of Pathway B, we observed a clear preference for one of the two isomeric transition states responsible for the regioselectivity of the reaction. The two saddle-points for the 1,3 O→N acyl transfer have nearly identical geometries and, again, they do not seem to differ with respect to steric interactions (Fig. 6). In this case, the significantly lower energy of $\mathbf{TS_{9\text{-}Ph}}$ is likely

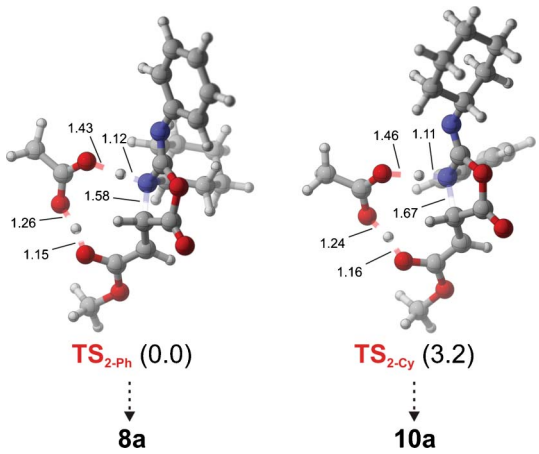

Fig. 5 Regioisomeric transition states for the aza-Michael cyclization. Relative energies are in kcal mol^{-1}.

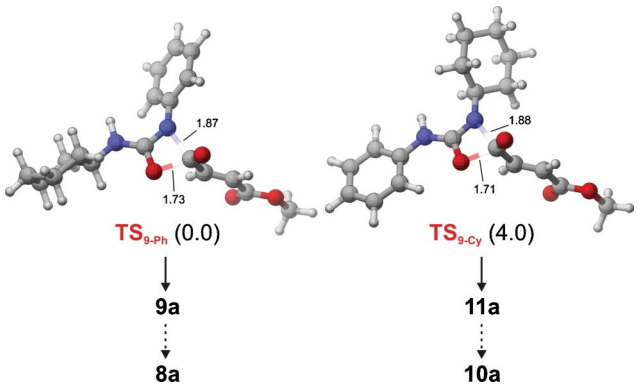

Fig. 6 Regioisomeric transition states for the 1,3 O→N acyl transfer.

the result of conjugation of the imine C═N bond with the phenyl substituent.

Next, we compared the overall barriers for product formation obtained using the larger model to the results previously obtained with compounds **1a** and **2**. These calculations confirmed the trend observed with the smaller model. In more detail, the overall barrier for Pathway A ($\mathbf{A_{Ph}}$→$\mathbf{TS_{2\text{-}Ph}}$) was found to be 29.6 kcal mol^{-1}, while the calculations indicate that Pathway B requires 26.4 kcal mol^{-1} ($\mathbf{K_{Ph}}$→$\mathbf{TS_{10\text{-}Ph}}$).

Therefore, B3LYP predicts that the formation of both products takes place through a common reaction pathway. Again, these results also indicate that generation of the previously postulated imino-oxazolidinone intermediate is energetically more demanding and might, therefore, not occur under the reaction conditions. On the other hand, in a recent report from these laboratories, we showed that α,β-unsaturated acids with higher Michael accepting capabilities react smoothly with carbodiimides and amines in a three-component one-pot transformation yielding urea-amides.[30] These products are likely to result from nucleophilic opening of an imino-oxazolidinone intermediate (similar to $\mathbf{TS_6}$ but with an amine rather than a carboxylate as nucleophile). Considering that variations of the substrate structure (*e.g.* by replacing alkyl ester with other electron-withdrawing groups) might significantly change the reactivity of the α,β-unsaturated acid component, both mechanistic hypotheses should be considered when studying related transformations.

Conclusions

The domino reaction between activated α,β-unsaturated carboxylic acids and carbodiimides has been scrutinized theoretically using the B3LYP and the MPW1K density functionals. Two alternative reaction pathways were taken into account using two different computational models.

The calculations indicate that both pathways have similar overall barriers. More specifically, B3LYP predicts a preference for a mechanism involving initial formation of an *O*-acyl isourea followed by *E*/*Z* isomerization and 1,3 O→N acyl transfer. The resulting *N*-acyl urea can subsequently undergo an intramolecular conjugate addition and tautomerization to the hydantoin product. On the other hand, MPW1K estimates the two pathways to have identical overall barriers. However, the qualitative predictions obtained using MPW1K with respect to the rate-determining steps do not match with the experimentally formed by-products.

In all the cases considered, inclusion of a second molecule of acid as proton shuttle and/or nucleophile was found to be crucial for the modeling. Calculations on an unsymmetrical carbodiimide correctly reproduced the experimentally observed regioselectivity. These results clearly indicate that the carboxylic acid serves the two-fold purpose of reactant and catalyst, a finding which could be exploited in the development of enantioselective versions of this transformation.

Acknowledgements

The authors gratefully acknowledge MIUR for financial support and CILEA for the generous allocation of computational resources

Notes and references

1 (*a*) Heterocycles and A. R. Katritzsky, *Chem. Rev.*, 2004, **104**, 2125 Ed; (*b*) A. F. Pozharskii, A. T. Soldatenkov, A. R. Katritzky, *Heterocyles in Life and Society*, Wiley, New York, 1997.

2 (*a*) J. C. Thenmozhiyal, P. T. H. Wong and W. K. Chui, *J. Med. Chem.*, 2004, **47**, 1527; (*b*) C. W. Bazil and T. A. Pedley, *Annu. Rev. Med.*, 1998, **49**, 135; (*c*) M. S. Luer, *Neurol. Res.*, 1998, **20**, 178; (*d*) M. Matsukara, Y. Daiku, K. Ueda, S. Tanaka, T. Igarashi and N. Minami, *Chem. Pharm. Bull.*, 1992, **40**, 1823; (*e*) J. Knabe, J. Baldauf and A. Ahlhelm, *Pharmazie*, 1997, **52**, 912; (*f*) L Somsá, L. Kovács, M. Tóth, E. Ősz, L. Szilágyi, Z. Györgydeák, Z. Dinya, T. Docsa, B. Tóth and P. Gergely, *J. Med. Chem.*, 2001, **44**, 2843; (*g*) G. P. Moloney, G. R. Martin, S. MacLennan, N. Mathews, S. Dosworth, P. Y. Sang, C. Knight and R. Glen, *J. Med. Chem.*, 1997, **40**, 2347; (*h*) M. Jansen, H. Potschka, C. Brandt, W. Loscher and G. Dannhardt, *J. Med. Chem.*, 2003, **46**, 64; (*i*) K. Last-Barney, W. Davidson, M. Cardozo, L. L. Frye, C. A. Grygon, J. L. Hopkins, D. D. Jeanfavre, S. Pav, C. Qian, J. M. Stevenson, L. Tong, R. Zindell and T. A. Kelly, *J. Am. Chem. Soc.*, 2001, **123**, 5643.

3 J. C. Sutherland and G. P. Hess, *Nat. Prod. Rep.*, 2000, **17**, 621.

4 (*a*) K. Yokozeki and K. Kubota, *Agric. Biol. Chem.*, 1987, **51**, 721–728; (*b*) M. B. Arcuri, O. A. C. Antunes, S. J. Sabino, G. F. Pinto and E. G. Oestreicher, *Amino Acids*, 2000, **19**, 477.

5 C. A. López and G. G. Trigo, *Adv. Heterocycl. Chem.*, 1985, **38**, 177.

6 A Boeijen, W. Kruijtzer and R. M. J. Liskamp, *Bioorg. Med. Chem. Lett.*, 1998, **8**, 2375.

7 M. Beller, M. Eckert, W. A. Moradi and H. Neumann, *Angew. Chem., Int. Ed.*, 1999, **38**, 1454.

8 C. Hulme, L. Ma, J. J. Romano, G. Morton, S. Y. Tang, M. P. Cherrier, S. Choi, J. Salvino and R. Labaudiniere, *Tetrahedron Lett.*, 2000, **41**, 1889.

9 M. Meusel, A. Ambrozak, T. K. Hecker and M. Gűtschow, *J. Org. Chem.*, 2003, **68**, 4684.

10 S. Hanessian and R. Y. Yang, *Tetrahedron Lett.*, 1996, **37**, 5835 and references cited therein.

11 (*a*) A. Volonterio and M. Zanda, *Tetrahedron Lett.*, 2003, **44**, 8549; (*b*) A. Volonterio, C. Ramirez de Arellano and M. Zanda, *J. Org. Chem.*, 2005, **70**, 2161.

12 M. J. Frisch, G. W. Trucks, H. B. Schlegel , G. E. Scuseria, M. A. Robb, J. R. Cheeseman, J. A. Montgomery Jr., T. Vreven, K. N. Kudin, J. C. Burant, J. M. Millam, S. S. Iyengar, J. Tomasi, V. Barone, B. Mennucci, M. Cossi, G. Scalmani, N. Rega, G. A. Petersson, H. Nakatsuji, M. Hada, M. Ehara, K. Toyota, R. Fukuda, J. Hasegawa, M. Ishida, T. Nakajima, Y. Honda, O. Kitao, H. Nakai, M. Klene, X. Li, J. E. Knox, H. P. Hratchian, J. B. Cross, C. Adamo, J. Jaramillo, R. Gomperts, R. E. Stratmann, O. Yazyev, A. J. Austin, R. Cammi, C. Pomelli, J. W. Ochterski, P. Y. Ayala, K. Morokuma, G. A. Voth, P. Salvador, J. J. Dannenberg, V. G. Zakrzewski, S. Dapprich, A. D. Daniels, M. C. Strain, O. Farkas, D. K. Malick, A. D. Rabuck, K. Raghavachari, J. B. Foresman, J. V. Ortiz, Q. Cui, A. G. Baboul, S. Clifford, J. Cioslowski, B. B. Stefanov, G. Liu, A. Liashenko, P. Piskorz, I. Komaromi, R. L. Martin, D. J. Fox, T. Keith, M. A. Al-Laham, C. Y. Peng, A. Nanayakkara, M. Challacombe, P. M. W. Gill, B. Johnson, W. Chen, M. W. Wong, C. Gonzalez and J. A. Pople, *Gaussian03*, revision C.02; Gaussian, Inc., Wallingford CT, 2004.

13 (*a*) C. Lee, W. Yang and R. G. Parr, *Phys. Rev. B*, 1988, **37**, 785; (*b*) A. D. Becke, *Phys. Rev. A*, 1988, **38**, 3098; (*c*) A. D. Becke, *J. Chem. Phys.*, 1992, **96**, 2155; (*d*) A. D. Becke, *J. Chem. Phys.*, 1992, **97**, 9173; (*e*) A. D. Becke, *J. Chem. Phys.*, 1993, **98**, 5648.

14 B. J. Lynch, P. L. Fast, M. Harris and D. G. Truhlar, *J. Phys. Chem. A*, 2000, **104**, 4811.

15 (*a*) M. Cossi, N. Rega, G. Scalmani and V. Barone, *J. Comput. Chem.*, 2003, **24**, 669; (*b*) V. Barone and M. Cossi, *J. Phys. Chem. A*, 1998, **102**, 1995.

16 C. Y. Legault, *CYLview*, 1.0b; Université de Sherbrooke, 2009 (http://www.cylview.org).

17 (*a*) T. Iwasawa, P. Wash, C. Gibson and J. Rebek Jr., *Tetrahedron*, 2007, **63**, 6506; (*b*) L. Bonsignore, F. Cottiglia, A. M. Maccioni, D. Secci and S. M. Lavagna, *J. Heterocycl. Chem.*, 1995, **32**, 573.

18 L. C. Chan and B. G. Cox, *J. Org. Chem.*, 2007, **72**, 8863.

19 W. T. Brady and R. A. Owens, *J. Org. Chem.*, 1977, **42**, 3220.

20 (*a*) D. Kim, Y. Kim and K. H. Kim, *J. Heterocycl. Chem.*, 1997, **34**, 311; (*b*) D. Kim, Y. Kim, J. Gam, J. Lim and K. H. Kim, *Tetrahedron Lett.*, 1995, **36**, 6257.

21 If the title reaction is performed in acetonitrile, we found that the *N*-acyl urea by-product can be readily cyclized at room temperature by addition of aqueous sodium hydroxide.

22 (*a*) M. Lewis and R. Glaser, *J. Am. Chem. Soc.*, 1998, **120**, 8541; (*b*) M. Lewis and R. Glaser, *Chem.–Eur. J.*, 2002, **8**, 1934; (*c*) M. T. Nguyen, G. Raspoet and L. G. Vanquickenborne, *J. Chem. Soc., Perkin Trans. 2*, 1999, 813.

23 (*a*) T. Marcelli and F. Himo, *Eur. J. Org. Chem.*, 2008, 4751; (*b*) G. O. Jones, X. Li, A. E. Hayden, K. N. Houk and S. J. Danishefsky, *Org. Lett.*, 2008, **10**, 4093.

24 (*a*) L. T. Nguyen, T. N. Le, F. De Proft, A. K. Chandra, W. Langenaeker, M. T. Nguyen and P. Geerlings, *J. Am. Chem. Soc.*, 1999, **121**, 5992; (*b*) M. T. Nguyen, A. V. Keer, K. Pierloot and L. G. Vanquickenborne, *J. Am. Chem. Soc.*, 1995, **117**, 7535; (*c*) M. T. Nguyen, A. F. Hegarty, M. Sana and G. Leroy, *J. Am. Chem. Soc.*, 1985, **107**, 4141; (*d*) M. T. Nguyen, T. Ha and A. F. Hegarty, *J. Phys. Org. Chem.*, 1990, **3**, 697.

25 This two-step sequence was found to be significantly more favoured compared to direct proton transfer to the α-carbon in the C–N bond forming step.

26 Y. Wei, B. Sateesh, B. Maryasin, G. N. Sastry and H. Zipse, *J. Comput. Chem.*, 2009, **30**, 2617.

27 N. Çelebi- Ölçüm, V. Aviyente and K. N. Houk, *J. Org. Chem.*, 2009, **74**, 6944.

28 This is observed experimentally in base-promoted cyclizations of *N*-acyl ureas, see ref. *14b*.

29 The stationary points for the larger model are arbitrarily named after the substituent ending on the imide nitrogen.

30 M. C. Bellucci and A. Volonterio, *Adv. Synth. Catal.*, 2010, **352**, 2791.